

## Constraints on New Physics in MFV models: a model-independent analysis of $\Delta F = 1$ processes

TOBIAS HURTH<sup>a,b</sup>, GINO ISIDORI<sup>c,d</sup>, JERNEJ F. KAMENIK<sup>d,e</sup>, FEDERICO MESCIA<sup>d</sup>

<sup>a</sup>*CERN, Dept. of Physics, Theory Division, CH-1211 Geneva, Switzerland*

<sup>b</sup>*SLAC, Stanford University, Stanford, CA 94309, USA*

<sup>c</sup>*Scuola Normale Superiore and INFN, Piazza dei Cavalieri 7, 56126 Pisa, Italy*

<sup>d</sup>*INFN, Laboratori Nazionali di Frascati, Via E. Fermi 40, I-00044 Frascati, Italy*

<sup>e</sup>*J. Stefan Institute, Jamova 39, P. O. Box 3000, 1001 Ljubljana, Slovenia*

### Abstract

We analyse the constraints on dimension-six  $\Delta F = 1$  effective operators in models respecting the MFV hypothesis, both in the one-Higgs doublet case and in the two-Higgs doublet scenario with large  $\tan\beta$ . The constraints are derived mainly from the  $b \rightarrow s$  inclusive observables measured at the  $B$  factories. The implications of these bounds in view of improved measurements in exclusive and inclusive observables in  $b \rightarrow s\ell^+\ell^-$  and  $s \rightarrow d\nu\bar{\nu}$  transitions are discussed.

# 1 Introduction

The Standard Model (SM) can be viewed as the renormalizable part of an effective field theory, valid up to some still undetermined cut-off scale  $\Lambda$  above the electroweak scale,  $(\sqrt{2}G_F)^{-1/2} \approx 250$  GeV. Theoretical arguments based on a natural solution of the hierarchy problem suggest that  $\Lambda$  should not exceed a few TeV. This expectation leads to a paradox when combined with the absence of significant deviations from the SM in loop-induced flavour-violating observables, potentially sensitive to very high energy scales. An effective solution to this problem is provided by the so-called hypothesis of Minimal Flavour Violation [1], namely by the assumption that the SM Yukawa couplings are the only relevant breaking sources of the  $SU(3)^5$  flavour symmetry [2] of the low-energy effective theory.<sup>1</sup>

This symmetry and symmetry-breaking ansatz is realised in various explicit extensions of the SM, such as supersymmetric models (see e.g. Ref [5, 6] and [7]) or models with extra dimensions (see e.g. Ref. [8]). However, its main virtue is the possibility to perform a general analysis of new-physics effects in low-energy observables independently of the ultraviolet completion of the model. As shown in Ref. [1], the MFV hypothesis allows to build a rather predictive effective theory in terms of SM and Higgs fields. The predictions on flavour-violating observables derived within this effective theory are powerful tests of the underlying flavour structure of the model: if falsified, these tests would unambiguously signal the presence of new symmetry-breaking terms.

The observables most relevant to test the MFV hypothesis and, within this framework, to constrain the structure of the effective theory are  $\Delta F = 2$  and  $\Delta F = 1$  flavour-changing neutral-current (FCNC) processes. An updated analysis of the  $\Delta F = 2$  sector, or the meson-antimeson mixing amplitudes, has been presented recently in Ref. [9]. The goal of this work is a complete analysis of the  $\Delta F = 1$  sector, or the rare-decay amplitudes.

Using the currently available measurements of  $\Delta F = 1$  FCNC processes from  $b \rightarrow s$  and  $s \rightarrow d$  transitions (see Table 1) we derive updated bounds on the effective scale of new physics within MFV models. We consider in particular both the scenario of one effective Higgs doublet and the case of two Higgs doublets and large  $\tan\beta$ , where we are free to change the relative normalization of the two Yukawa couplings and to decouple the breaking of  $U(1)_{PQ}$  and  $SU(3)^5$  global symmetries [1].

Having derived the bounds on the effective operators from the observables listed in Table 1, we derive a series of predictions for exclusive and inclusive observables in  $b \rightarrow s\ell^+\ell^-$  and  $s \rightarrow d\nu\bar{\nu}$  transitions which have not been measured so far with high accuracy. On the one hand, these predictions indicate where to look for large new physics effects in the flavour sector, even under the pessimistic hypothesis of MFV. On the other hand, some of these predictions could provide, in the future, a proof of the MFV hypothesis: a set of deviations from the SM exhibiting the correlation predicted by this symmetry structure.

The paper is organised as follows: in Section 2 we review the structure of the effective  $\Delta F = 1$  Hamiltonian under the MFV hypothesis. The theoretical expressions of the observables analysed, in terms of the Wilson coefficients of the effective theory, are presented in Section 3. The numerical bounds on the scale of new physics and the predictions for future measurements are discussed in Section 4 and 5, respectively. The results are briefly summarised in the Conclusions.

---

<sup>1</sup> For earlier/alternative definitions of the MFV hypothesis see Ref. [3, 4].

Observable	Experiment	SM prediction
$\mathcal{B}(B \rightarrow X_s \gamma)_{[E_\gamma > 1.6 \text{ GeV}]}$	$(3.52 \pm 0.24) \times 10^{-4}$ [10]	$(3.13 \pm 0.23) \times 10^{-4}$ [11–13]
$\mathcal{B}(B \rightarrow X_s \ell^+ \ell^-)_{[q^2 \in [0.04, 1.0] \text{ GeV}^2]}$	$(0.6 \pm 0.5) \times 10^{-6}$	$(0.8 \pm 0.2) \times 10^{-6}$
$\mathcal{B}(B \rightarrow X_s \ell^+ \ell^-)_{[q^2 \in [1.0, 6.0] \text{ GeV}^2]}$	$(1.6 \pm 0.5) \times 10^{-6}$ [14, 15] <sup>a</sup>	$(1.6 \pm 0.1) \times 10^{-6}$ [16–23]
$\mathcal{B}(B \rightarrow X_s \ell^+ \ell^-)_{[q^2 > 14.4 \text{ GeV}^2]}$	$(4.4 \pm 1.3) \times 10^{-7}$	$(2.4 \pm 0.8) \times 10^{-7}$
$\mathcal{B}(B_s \rightarrow \mu^+ \mu^-)$	$< 5.8 \times 10^{-8}$ (95% CL) [24]	$(4.1 \pm 0.8) \times 10^{-9}$ [25, 26]
$\bar{A}_{FB}(B \rightarrow K^* \ell^+ \ell^-)_{[q^2 < 6.25 \text{ GeV}^2]}$	$0.24^{+0.19}_{-0.24}$	$-0.01 \pm 0.02$
$\bar{A}_{FB}(B \rightarrow K^* \ell^+ \ell^-)_{[q^2 > 10.24 \text{ GeV}^2]}$	$0.76^{+0.53}_{-0.34}$ [27]	$0.20 \pm 0.08$ [28–31]
$\mathcal{B}(K^+ \rightarrow \pi^+ \nu \bar{\nu})$	$(14.7^{+13.0}_{-8.9}) \times 10^{-11}$ [32]	$(8.6 \pm 0.9) \times 10^{-11}$ [33–37]

<sup>a</sup>Here we quote naïve averages of the values obtained by the experiments and with symmetrized errors.

Table 1: Main observables used to determine bounds on the MFV dimension-six operators. The SM predictions are updated according to the most recent determinations of the SM input values (see Section 4).

## 2 MFV and $\Delta F = 1$ processes

Under the MFV hypothesis, the dimension-six effective operators relevant to down-type FCNC transitions, both with one or two Higgs doublets, can be defined as follows [1]:

$$\begin{aligned}
\mathcal{O}_{H1} &= i (\bar{Q}_L \lambda_{\text{FC}} \gamma_\mu Q_L) H_U^\dagger D_\mu H_U, & \mathcal{O}_{H2} &= i (\bar{Q}_L \lambda_{\text{FC}} \tau^a \gamma_\mu Q_L) H_U^\dagger \tau^a D_\mu H_U, \\
\mathcal{O}_{G1} &= H_D (\bar{Q}_L \lambda_{\text{FC}} \lambda_d \sigma_{\mu\nu} T^a D_R) (g_s G_{\mu\nu}^a), & \mathcal{O}_{G2} &= (\bar{Q}_L \lambda_{\text{FC}} \gamma_\mu T^a Q_L) (g_s D_\mu G_{\mu\nu}^a), \\
\mathcal{O}_{F1} &= H_D (\bar{Q}_L \lambda_{\text{FC}} \lambda_d \sigma_{\mu\nu} D_R) (e F_{\mu\nu}), & \mathcal{O}_{F2} &= (\bar{Q}_L \lambda_{\text{FC}} \gamma_\mu Q_L) (e D_\mu F_{\mu\nu}), \\
\mathcal{O}_{\ell 1} &= (\bar{Q}_L \lambda_{\text{FC}} \gamma_\mu Q_L) (\bar{L}_L \gamma_\mu L_L), & \mathcal{O}_{\ell 2} &= (\bar{Q}_L \lambda_{\text{FC}} \gamma_\mu \tau^a Q_L) (\bar{L}_L \gamma_\mu \tau^a L_L), \\
\mathcal{O}_{\ell 3} &= (\bar{Q}_L \lambda_{\text{FC}} \gamma_\mu Q_L) (\bar{E}_R \gamma_\mu E_R), & \mathcal{O}_{S1} &= (\bar{Q}_L \lambda_{\text{FC}} \lambda_d D_R) (\bar{E}_R \lambda_\ell L_L).
\end{aligned} \tag{1}$$

The five fermion fields ( $Q_L$ ,  $D_R$ ,  $U_R$ ,  $L_L$ ,  $E_R$ ) carry a flavour index ( $i = 1, \dots, 3$ ): since we are interested in FCNC processes of down-type quarks, it is convenient to work in the mass-eigenstate basis of charged leptons and down-type quarks, where  $\lambda_{d,\ell} = \text{diag}\{m_{d,\ell}/\langle H_D \rangle\}$ . In this basis the flavour-changing coupling  $(\lambda_{\text{FC}})_{ij}$  can be expanded as

$$(\lambda_{\text{FC}}) = \begin{cases} (Y_U Y_U^\dagger)_{ij} \approx \lambda_t^2 V_{3i}^* V_{3j} & i \neq j, \\ 0 & i = j, \end{cases} \tag{2}$$

in terms of the top-quark Yukawa coupling ( $\lambda_t = m_t/\langle H_U \rangle \approx 1$ ) and the CKM matrix ( $V_{ij}$ ). Note that we have defined the operators linear in the gauge fields including appropriate powers of the corresponding gauge couplings (contrary to the original definition of Ref. [1]). Moreover, we have included from the beginning the scalar-density operator  $\mathcal{O}_{S1}$ , which plays a relevant role in the two-Higgs doublet case at large  $\tan \beta = \langle H_U \rangle / \langle H_D \rangle$ .<sup>2</sup> For all the operators linear in  $\lambda_d$  we could also consider a corresponding set with opposite chirality ( $D_R \leftrightarrow Q_L$ ); however, the hierarchical structure of  $\lambda_d$  implies that only one chirality structure is relevant. In the following we restrict the attention to flavour transitions of the type  $j > i$ , such as the leading chirality structure is the one in Eq. (1).

<sup>2</sup> In principle, in the two-Higgs doublet case we can consider additional operators obtained from those in (1) by the exchange  $H_U \rightarrow H_D$  and/or  $\lambda_{\text{FC}} \rightarrow Y_D Y_D^\dagger \lambda_{\text{FC}}$ . However, for all the B physics observables we analyse in this work, the effects of these additional operators can be reabsorbed into a redefinition of the couplings of the operators in (1).

Before the breaking of the electroweak symmetry, we define the MFV effective Lagrangian as  $\mathcal{L}_{\text{eff-MFV}}^{\Delta F=1} = (\sum_n a_n \mathcal{O}_n)/\Lambda^2$ , where  $a_i$  are  $O(1)$  couplings and  $\Lambda$  is the effective scale of new physics. After the spontaneous breaking of the electroweak symmetry, the operators in (1) are mapped onto the standard basis of FCNC operators, defined by

$$\mathcal{H}_{\text{eff}}^{\Delta F=1} = -\frac{G_F \alpha_{\text{em}}}{2\sqrt{2}\pi \sin^2 \theta_W} V_{3i}^* V_{3j} \sum_n C_n^{\text{MFV}} \mathcal{Q}_n + \text{h.c.}, \quad (3)$$

where

$$\begin{aligned} \mathcal{Q}_7 &= \frac{e}{g^2} m_j \bar{d}_i \sigma_{\mu\nu} (1 + \gamma_5) d_j F_{\mu\nu}, & \mathcal{Q}_8 &= \frac{g_s}{g^2} m_j \bar{d}_i \sigma_{\mu\nu} T^a (1 + \gamma_5) d_j G_{\mu\nu}^a, \\ \mathcal{Q}_9 &= \bar{d}_i \gamma_\mu (1 - \gamma_5) d_j \sum_\ell \bar{\ell} \gamma_\mu \ell, & \mathcal{Q}_{10} &= \bar{d}_i \gamma_\mu (1 - \gamma_5) d_j \sum_\ell \bar{\ell} \gamma_\mu \gamma_5 \ell, \\ \mathcal{Q}_{\nu\bar{\nu}} &= \bar{d}_i \gamma_\mu (1 - \gamma_5) d_j \sum_\nu \bar{\nu} \gamma_\mu (1 - \gamma_5) \nu, & \mathcal{Q}_S^\ell &= \bar{d}_i (1 + \gamma_5) d_j \bar{\ell} (1 - \gamma_5) \ell. \end{aligned} \quad (4)$$

Defining

$$\epsilon_i = \left(\frac{\Lambda_0}{\Lambda}\right)^2 a_i, \quad \Lambda_0 = \frac{\lambda_t \sin^2 \theta_W m_W}{\alpha_{\text{em}}} \approx 2.4 \text{ TeV}, \quad (5)$$

the modified initial conditions of the Wilson coefficients of this effective Hamiltonian at the electroweak scale,  $\delta C_i = C_i^{\text{MFV}}(\mu_H) - C_i^{\text{SM}}(\mu_H)$ , are [1]

$$\begin{aligned} \delta C_7 &= 2g^2 \epsilon_{F1}, & \delta C_8 &= 2g^2 \epsilon_{G1}, \\ \delta C_9 &= \epsilon_{\ell 1} + \epsilon_{\ell 2} + \epsilon_{\ell 3} - [(1 - 4 \sin^2 \theta_W) \epsilon_Z + 2e^2 \epsilon_{F2}], & \delta C_{10} &= \epsilon_Z - \epsilon_{\ell 1} - \epsilon_{\ell 2} + \epsilon_{\ell 3}, \\ \delta C_S^\ell &= \lambda_{d_j} \lambda_\ell \epsilon_{S1}, & \delta C_{\nu\bar{\nu}} &= \epsilon_Z + \epsilon_{\ell 1} - \epsilon_{\ell 2}, \end{aligned} \quad (6)$$

where  $\epsilon_Z = (\epsilon_{H1} + \epsilon_{H2})/2$ .

At this point it is useful to compare our effective  $\Delta F = 1$  Hamiltonian to those adopted in similar analyses in the recent literature. Bounds on the scale of new physics and corresponding predictions for rare decays in MFV scenarios have been discussed also by other authors (see e.g. Ref. [38–40]). However, most of the recent analyses concentrated on a specific version of the general MFV framework [1], the so-called *constrained* MFV (CMFV) [3]. While MFV as proposed in [1] is an hypothesis about the symmetry-breaking structure of the  $SU(3)^5$  flavour symmetry, the CMFV contains a further dynamical assumption: the hypothesis of no new effective dimension-six flavour-changing operators beside the SM ones (after electroweak symmetry breaking). In practice, also this dynamical assumption can be related to a symmetry-breaking issue: namely the hypothesis about the breaking of the  $U(1)_{\text{PQ}}$  symmetry of the SM gauge Lagrangian [1]. Indeed independently from the value of  $\tan \beta = \langle H_U \rangle / \langle H_D \rangle$ , in absence of a sizable  $U(1)_{\text{PQ}}$  breaking the coefficient of the scalar operator is too small to compensate the strong  $\lambda_{d_j} \lambda_\ell$  suppression in Eq. (6). Since large  $U(1)_{\text{PQ}}$  breakings can occur in well-motivated extensions of the SM, such as supersymmetric models (see e.g. [41–43]), we make no specific assumptions about its size and take into account also the effects of the scalar operators. For the same reason, using the definition of  $\lambda_{\text{FC}}$  in (2) we remove from the operator basis terms contributing to flavour-conserving processes induced by the diagonal component of  $Y_U Y_U^\dagger$ . At large  $\tan \beta$  flavour-diagonal terms could receive additional contributions of the type  $Y_D Y_D^\dagger$ , therefore we cannot use them to bound the flavour-changing terms. This does not occur in the CMFV, where  $Z \rightarrow b\bar{b}$  provide a useful constraint on flavour-changing operators [40].

## 2.1 Effective weak Hamiltonian at $\mu = m_b$

When computing  $\Delta F = 1$  observables, we need to take into account also the contributions of four-quark operators. Following the notation of Ref. [16], we write the complete effective Hamiltonian

relevant to  $b \rightarrow s$  transitions as

$$\begin{aligned} \mathcal{H}_{\text{eff}}^{b \rightarrow s} &= -\frac{4G_F}{\sqrt{2}} [V_{us}^* V_{ub} (C_1^c P_1^u + C_2^c P_2^u) + V_{cs}^* V_{cb} (C_1^c P_1^c + C_2^c P_2^c)] \\ &- \frac{4G_F}{\sqrt{2}} \left\{ \sum_{i=3}^{10} [(V_{us}^* V_{ub} + V_{cs}^* V_{cb}) C_i^c + V_{ts}^* V_{tb} C_i^t] P_i + V_{ts}^* V_{tb} C_0^\ell P_0^\ell \right\} + \text{h.c.}, \end{aligned} \quad (7)$$

where

$$\begin{aligned} P_1^u &= (\bar{s}_L \gamma_\mu T^a u_L) (\bar{u}_L \gamma^\mu T^a b_L), & P_5 &= (\bar{s}_L \gamma_{\mu_1} \gamma_{\mu_2} \gamma_{\mu_3} b_L) \sum_q (\bar{q} \gamma^{\mu_1} \gamma^{\mu_2} \gamma^{\mu_3} q), \\ P_2^u &= (\bar{s}_L \gamma_\mu u_L) (\bar{u}_L \gamma^\mu b_L), & P_6 &= (\bar{s}_L \gamma_{\mu_1} \gamma_{\mu_2} \gamma_{\mu_3} T^a b_L) \sum_q (\bar{q} \gamma^{\mu_1} \gamma^{\mu_2} \gamma^{\mu_3} T^a q), \\ P_1^c &= (\bar{s}_L \gamma_\mu T^a c_L) (\bar{c}_L \gamma^\mu T^a b_L), & P_7 &= \frac{e}{g_s^2} m_b (\bar{s}_L \sigma^{\mu\nu} b_R) F_{\mu\nu}, \\ P_2^c &= (\bar{s}_L \gamma_\mu c_L) (\bar{c}_L \gamma^\mu b_L), & P_8 &= \frac{1}{g_s} m_b (\bar{s}_L \sigma^{\mu\nu} T^a b_R) G_{\mu\nu}^a, \\ P_3 &= (\bar{s}_L \gamma_\mu b_L) \sum_q (\bar{q} \gamma^\mu q), & P_{10} &= \frac{e^2}{g_s^2} (\bar{s}_L \gamma_\mu b_L) \sum_\ell (\bar{\ell} \gamma^\mu \gamma_5 \ell), \\ P_4 &= (\bar{s}_L \gamma_\mu T^a b_L) \sum_q (\bar{q} \gamma^\mu T^a q), & P_9 &= \frac{e^2}{g_s^2} (\bar{s}_L \gamma_\mu b_L) \sum_\ell (\bar{\ell} \gamma^\mu \ell). \end{aligned} \quad (8)$$

With respect to the SM literature we also add the scalar-density operator with right-handed  $b$  quark,

$$P_0^\ell = \frac{e^2}{16\pi^2} (\bar{s}_L b_R) (\bar{\ell}_R \ell_L), \quad (9)$$

which plays an important role in the large  $\tan \beta$  regime. This operator is present also in the SM, but it is usually neglected because of the strong suppression of its Wilson coefficients.

In principle we should consider new-physics effects both in the four-quark ( $P_{1-6}$ ) and in the FCNC operators. However, four-quark operators receive a large SM contribution which is naturally much larger with respect to the new-physics one in the MFV scenario. Moreover four-quark operators do not contribute at the tree-level to the observables we are considering (FCNC processes). As a result, it is a good approximation to consider new-physics effects only in the leading FCNC operators:<sup>3</sup>

$$\begin{aligned} C_7^t(\mu_H) &= C_{7,SM}^t(\mu_H) + \frac{\alpha_s}{4\pi} \delta C_7, \\ C_8^t(\mu_H) &= C_{8,SM}^t(\mu_H) + \frac{\alpha_s}{4\pi} \delta C_8, \\ C_9^t(\mu_H) &= C_{9,SM}^t(\mu_H) + \frac{\alpha_s}{4\pi \sin^2 \theta_W} \delta C_9, \\ C_{10}^t(\mu_H) &= C_{10,SM}^t(\mu_H) + \frac{\alpha_s}{4\pi \sin^2 \theta_W} \delta C_{10}, \\ C_0^\ell(\mu_H) &= \frac{2}{\sin^2 \theta_W} \delta C_S^\ell, \end{aligned} \quad (10)$$

with the  $\delta C_i$  given in Eq. (6). The initial conditions for the SM terms are obtained by a NNLO matching of the effective Wilson coefficients at the high scale  $\mu_H \in [80, 160]$  GeV, using CKM unitarity to get rid of  $V_{cb}^* V_{cs} / V_{tb}^* V_{ts}$  [16].

---

<sup>3</sup> Even including explicit new-physics contributions to  $C_{1-6}$ , to an excellent accuracy these could be reabsorbed into the Wilson coefficients of the FCNC operators.

Quantity	Value
$\sin^2 \theta_W$	0.2312
$\alpha_s(m_Z)$	0.1187
$\alpha_{\text{em}}(m_Z)$	1/127.8
$m_b^{MS}(m_b)$	4.2 GeV
$m_t^{MS}(m_t)$	165 GeV

Table 2: Reference input values used in the matching and in the RGE evolution of the Wilson coefficients.

To a good approximation, in all the considered low-energy observables  $\delta C_7$  and  $\delta C_8$  appear in a fixed linear combination:

$$\delta C_7 + 0.3 \delta C_8 . \quad (11)$$

For this reason, in the following we set  $\delta C_8 = 0$  and treat only  $\delta C_7$  as independent fit parameter (avoiding the flat direction in the parameter space determined by Eq. (11)). The bounds on  $\delta C_7$  thus obtained should therefore be interpreted as bounds on the  $\delta C_7$ - $\delta C_8$  combination in Eq. (11).

The Wilson coefficients are evolved from the high scale down to  $\mu_b = O(m_b)$  using SM renormalization group equations at the NNLO accuracy [44, 45]. At the low scale it is convenient to define the effective coefficients [18]

$$A_7 = \frac{4\pi}{\alpha_s(\mu_b)} C_7(\mu_b) - \frac{1}{3} C_3(\mu_b) - \frac{4}{9} C_4(\mu_b) - \frac{20}{3} C_5(\mu_b) - \frac{80}{9} C_6(\mu_b), \quad (12)$$

$$A_9 = \frac{4\pi}{\alpha_s(\mu_b)} C_9(\mu_b) + \sum_{i=1}^6 C_i(\mu_b) \gamma_{i9}^{(0)} \ln \frac{m_b}{\mu} + \frac{4}{3} C_3(\mu_b) + \frac{64}{9} C_5(\mu_b) + \frac{64}{27} C_6(\mu_b), \quad (13)$$

$$A_{10} = \frac{4\pi}{\alpha_s(\mu_b)} C_{10}(\mu_b), \quad (14)$$

$$T_9 = \frac{4}{3} C_1(\mu_b) + C_2(\mu_b) + 6 C_3(\mu_b) + 60 C_5(\mu_b), \quad (15)$$

$$U_9 = -\frac{7}{2} C_3(\mu_b) - \frac{2}{3} C_4(\mu_b) - 38 C_5(\mu_b) - \frac{32}{3} C_6(\mu_b), \quad (16)$$

$$W_9 = -\frac{1}{2} C_3(\mu_b) - \frac{2}{3} C_4(\mu_b) - 8 C_5(\mu_b) - \frac{32}{3} C_6(\mu_b), \quad (17)$$

where  $C_i(\mu) = C_i^t(\mu) - C_i^c(\mu)$ ,  $\gamma_{i9}^{(0)}$  is given in [16] and we have neglected the tiny  $u$ -quark loop contribution to  $A_9$ . The reference input values used in this procedure are collected in Table 2.

Beside  $B$  physics, we are interested also in  $s \rightarrow d$  transitions and particularly in the rare decays  $K \rightarrow \pi \nu \bar{\nu}$ . In the MFV framework these are described by the following simple effective Hamiltonian

$$\mathcal{H}_{\text{eff}}^{s \rightarrow d} = \frac{G_F \alpha_{\text{em}}(m_Z)}{\sqrt{2}} \sum_{\ell=e,\mu,\tau} \left( \frac{y_\nu}{2\pi \sin^2 \theta_W} P_{\nu \bar{\nu}} \right) + \text{h.c.} , \quad (18)$$

where

$$P_{\nu \bar{\nu}} = (\bar{s} \gamma_\mu d) (\bar{\nu}_\ell \gamma^\mu (1 - \gamma_5) \nu_\ell) , \quad (19)$$

$$y_\nu = \frac{1}{|V_{us}|} \left( \lambda_t (X_t + \delta C_{\nu \bar{\nu}}) + \text{Re} \lambda_c \tilde{P}_{u,c} \right) , \quad (20)$$

with  $\lambda_q = V_{qs}^* V_{qd}$ ,  $X_t = 1.464 \pm 0.041$ ,  $\tilde{P}_{u,c} = (0.2248)^4 P_{u,c}$  [33] and  $P_{u,c} = 0.41 \pm 0.04$  [34–36].

### 3 Observables

The observables we are interested in, either to derive bounds from the existing measurements or to obtain predictions for future measurements, are the differential decay distributions of  $B \rightarrow X_s \ell^+ \ell^-$  and  $B \rightarrow (K^*, K) \ell^+ \ell^-$  decays, and the integrated rates of  $B_{s,d} \rightarrow \ell^+ \ell^-$ ,  $B \rightarrow X_s \gamma$ ,  $B \rightarrow K^{(*)} \nu \bar{\nu}$  and  $K \rightarrow \pi \nu \bar{\nu}$ . In the following we analyse the theoretical expressions of these observables in terms of the (non-standard) Wilson coefficients of the MFV effective theory.

#### 3.1 $B \rightarrow X_s \ell^+ \ell^-$

In order to minimise the theoretical uncertainty, we normalise all the observables to the corresponding SM predictions. The numerical values for the SM predictions are computed at full NNLO accuracy, applying also QED corrections, following the analysis of Ref. [21, 22], and non-perturbative  $1/m_b$  corrections [19, 23]. On the other hand, since full NNLO expressions for the non-standard operator basis in (7) are not available, the relative deviations from the SM are computed at NLO accuracy (with partial inclusion of NNLO corrections, as discussed below). Given the overall good agreement between data and SM predictions, and the corresponding smallness of non-standard effects, this procedure minimise the theoretical uncertainty.

Following the standard notations of  $B \rightarrow X_s \ell^+ \ell^-$  analyses within the SM, we define the effective coefficients

$$\tilde{C}_7^{\text{eff}} = \left[ 1 + \frac{\alpha_s}{\pi} \omega_7(\hat{s}) \right] A_7 + \dots, \quad (21a)$$

$$\tilde{C}_9^{\text{eff}} = \left[ 1 + \frac{\alpha_s}{\pi} \omega_9(\hat{s}) \right] [A_9 + T_9 h(\hat{m}_c^2, \hat{s}) + U_9 h(1, \hat{s}) + W_9 h(0, \hat{s})] + \dots, \quad (21b)$$

$$\tilde{C}_{10}^{\text{eff}} = \left[ 1 + \frac{\alpha_s}{\pi} \omega_9(\hat{s}) \right] A_{10} + \dots, \quad (21c)$$

where all quantities with a hat are normalized to the  $b$  quark pole mass ( $\hat{x} = x/m_b$ ). The leading-order gluon bremsstrahlung corrections  $\omega_i(\hat{s})$  and the loop function  $h(x, y)$  can be found in [18, 19], while the dots denote additional perturbative  $\alpha_s$  and electro-magnetic corrections, as well as non-perturbative power corrections, which we only consider for the SM normalization. The Wilson coefficients are evolved down to the low scale  $\mu_b = 2.5$  GeV, using the input values in Table 2. As shown in [19], using such a low renormalisation scale minimise the NNLO QCD corrections to the  $B \rightarrow X_s \ell^+ \ell^-$  differential rate. An important difference with respect to the SM case is the presence of the  $P_0^\ell$  operator. To the level of accuracy we are working at, its inclusion is straightforward, since it is renormalised only in a multiplicative way.

We are now ready to compute the inclusive decay spectra. Neglecting the strange quark mass while keeping the full dependence on the lepton mass, we get for the unnormalized forward-

backward asymmetry and the rate

$$\begin{aligned} \frac{dA_{FB}}{d\hat{s}} &= \frac{G_F^2 \alpha_{\text{em}}^2 m_b^5}{256\pi^5} |V_{tb} V_{ts}^*|^2 (1 - \hat{s})^2 \left(1 - \frac{4\hat{m}_\ell^2}{\hat{s}^2}\right) \\ &\times \left\{ -2\text{Re} \left( \tilde{C}_9^{\text{eff}} \tilde{C}_{10}^{\text{eff}*} \right) \hat{s} - 4\text{Re} \left( \tilde{C}_7^{\text{eff}} \tilde{C}_{10}^{\text{eff}*} \right) + \text{Re} \left( \tilde{C}_9^{\text{eff}} C_0^{\ell*} \right) \hat{m}_\ell + 2\text{Re} \left( \tilde{C}_7^{\text{eff}} C_0^{\ell*} \right) \hat{m}_\ell \right\}, \end{aligned} \quad (22)$$

$$\begin{aligned} \frac{d\Gamma}{d\hat{s}} &= \frac{G_F^2 \alpha_{\text{em}}^2 m_b^5}{768\pi^5} |V_{tb} V_{ts}^*|^2 (1 - \hat{s})^2 \sqrt{1 - \frac{4\hat{m}_\ell^2}{\hat{s}^2}} \\ &\times \left\{ \left[ 12\text{Re}(\tilde{C}_7^{\text{eff}} \tilde{C}_9^{\text{eff}*}) + \frac{4|\tilde{C}_7^{\text{eff}}|^2(2 + \hat{s})}{\hat{s}} \right] \left(1 + \frac{2\hat{m}_\ell^2}{\hat{s}}\right) + 6\hat{m}_\ell^2(|\tilde{C}_9^{\text{eff}}|^2 - |\tilde{C}_{10}^{\text{eff}}|^2) \right. \\ &+ (|\tilde{C}_9^{\text{eff}}|^2 + |\tilde{C}_{10}^{\text{eff}}|^2) \left[ 1 + 2\hat{s} + \frac{2\hat{m}_\ell^2(1 - \hat{s})}{\hat{s}} \right] + \frac{3}{4}\hat{s} \left[ \left(1 - \frac{4\hat{m}_\ell^2}{\hat{s}}\right) |C_0^\ell|^2 \right] \\ &\left. + 3\hat{m}_\ell \text{Re}(C_0^\ell \tilde{C}_{10}^{\text{eff}*}) \right\}. \end{aligned} \quad (23)$$

As anticipated, these expressions are used only to evaluate the relative impact of new physics. Altogether, the estimated theoretical errors for the integrated inclusive rates reported in Table 1 are around 10%–30%. In the numerical analysis this error is added in quadrature to the experimental one, which, at present, provides the largely dominant source of uncertainty.<sup>4</sup>

### 3.2 $B \rightarrow (K^*, K)\ell^+\ell^-, B \rightarrow (K^*, K)\nu\bar{\nu}$

Exclusive modes are affected by a substantially larger theoretical uncertainty with respect to the inclusive ones. However, they are experimentally easier and allow to probe or constrain combinations of Wilson coefficients which are not accessible (or hardly accessible) in the inclusive modes. The most interesting observables for our analysis are the forward-backward asymmetry (FBA) in  $B \rightarrow K^*\ell^+\ell^-$  and the lepton universality ratio in  $B \rightarrow K^{(*)}\ell^+\ell^-$ . In addition, interesting predictions can be derived for the  $B \rightarrow (K^*, K)\nu\bar{\nu}$  decay rates.

In the  $B \rightarrow K^*\ell^+\ell^-$  case we need to introduce seven independent hadronic form factors ( $V$ ,

---

<sup>4</sup> There are two sources of theoretical uncertainties which, at present, are difficult to estimate: i) non-perturbative power corrections of order  $\alpha_s \Lambda/m_b$ ; ii) radiative corrections associated to the soft-photon experimental cuts applied in the experiments. In the first case the effect is estimated to be of  $O(5\%)$  by simple dimensional counting [46] (more sophisticated estimates using the vacuum insertion method in the context of  $B \rightarrow X_s \gamma$  confirm this naive estimate [47]). As far as radiative corrections are concerned, the theoretical predictions include a correction due to collinear logs [22] which does not correspond to the treatment of soft and collinear photons performed so far by the experiments [48]. We guesstimate this mismatch as a 10% uncertainty in the high- $q^2$  region and 5% error in the low- $q^2$  region. Given the large experimental uncertainties, which are still dominant, the impact of these additional theory errors turns out to be negligible. However, we stress that in the future a reduction of the theory uncertainties can be obtained only with a proper treatment of soft-photon corrections.



$A_{0-2}, T_{1-3}$  [31, 49]). Following Refs. [50, 51] we define the following set of auxiliary variables:

$$\begin{aligned}
A(\hat{s}) &= \frac{2}{1 + \hat{m}_{K^*}} C_9^{\text{eff}}(\hat{s}) V(\hat{s}) + \frac{4\hat{m}_b}{\hat{s}} C_7^{\text{eff}} T_1(\hat{s}) , \\
B(\hat{s}) &= (1 + \hat{m}_{K^*}) \left[ C_9^{\text{eff}}(\hat{s}) A_1(\hat{s}) + \frac{2\hat{m}_b}{\hat{s}} (1 - \hat{m}_{K^*}) C_7^{\text{eff}} T_2(\hat{s}) \right] , \\
C(\hat{s}) &= \frac{1}{1 - \hat{m}_{K^*}^2} \left[ (1 - \hat{m}_{K^*}) C_9^{\text{eff}}(\hat{s}) A_2(\hat{s}) + 2\hat{m}_b C_7^{\text{eff}} \left( T_3(\hat{s}) + \frac{1 - \hat{m}_{K^*}^2}{\hat{s}} T_2(\hat{s}) \right) \right] , \\
D(\hat{s}) &= \frac{1}{\hat{s}} \left[ C_9^{\text{eff}}(\hat{s}) ((1 + \hat{m}_{K^*}) A_1(\hat{s}) - (1 - \hat{m}_{K^*}) A_2(\hat{s}) - 2\hat{m}_{K^*} A_0(\hat{s})) - 2\hat{m}_b C_7^{\text{eff}} T_3(\hat{s}) \right] , \\
E(\hat{s}) &= \frac{2}{1 + \hat{m}_{K^*}} C_{10}^{\text{eff}} V(\hat{s}) , \\
F(\hat{s}) &= (1 + \hat{m}_{K^*}) C_{10}^{\text{eff}} A_1(\hat{s}) , \\
G(\hat{s}) &= \frac{1}{1 + \hat{m}_{K^*}} C_{10}^{\text{eff}} A_2(\hat{s}) , \\
H(\hat{s}) &= \frac{1}{\hat{s}} C_{10}^{\text{eff}} [(1 + \hat{m}_{K^*}) A_1(\hat{s}) - (1 - \hat{m}_{K^*}) A_2(\hat{s}) - 2\hat{m}_{K^*} A_0(\hat{s})] , \\
X(\hat{s}) &= -\frac{m_{K^*}}{m_b} A_0(\hat{s}) C_0^\ell , \tag{24}
\end{aligned}$$

where now all quantities with a hat are normalized to the physical meson mass (and bremsstrahlung corrections are omitted from the effective Wilson coefficients without the tilde). Also in this case the above expressions are used only to evaluate deviations from the SM. As far as the SM predictions are concerned, in this case the most accurate results are obtained by means of QCD factorisation and SCET [28–30, 52, 53]. However, here we adopt a conservative point of view and evaluate the SM predictions and the corresponding errors by means of the parametrisation and QCD SR calculations of Ref. [31]. Then we enlarge the theoretical errors by the differences between our SM predictions and known QCD factorization and SCET results [28–30]. In practice, given the large experimental errors, this choice has almost no influence on the constraints derived.

Using the auxiliary variables in Eq. (24), the un-normalised FBA then reads

$$\begin{aligned}
\frac{d\mathcal{A}_{\text{FB}}}{d\hat{s}} &= \frac{G_F^2 \alpha_{\text{em}}^2 m_B^5}{2^{10} \pi^5} |V_{ts}^* V_{tb}|^2 \hat{u}(\hat{s})^2 \times \\
&\times \left\{ \hat{s} \text{Re}(BE^*) + \hat{s} \text{Re}(AF^*) - \frac{\hat{m}_\ell}{\hat{m}_{K^*}^2} [\lambda \text{Re}(XC^*) - (1 - \hat{m}_{K^*}^2 - \hat{s}) \text{Re}(XB^*)] \right\} , \tag{25}
\end{aligned}$$

where

$$\hat{u}(\hat{s}) = \sqrt{\lambda \left( 1 - 4 \frac{\hat{m}_\ell^2}{\hat{s}} \right)} , \tag{26}$$

$$\lambda \equiv \lambda(1, \hat{m}_{K^*}^2, \hat{s}) = 1 + \hat{m}_{K^*}^4 + \hat{s}^2 - 2\hat{s} - 2\hat{m}_{K^*}^2(1 + \hat{s}) . \tag{27}$$

Similarly the decay rate can be written as

$$\begin{aligned}
\frac{d\Gamma}{d\hat{s}} = & \frac{G_F^2 \alpha_{\text{em}}^2 m_B^5}{2^{10} \pi^5} |V_{ts}^* V_{tb}|^2 \times \left\{ \frac{|A|^2}{3} \lambda (\hat{s} + \hat{m}_\ell^2) + \frac{|E|^2}{3} \lambda (\hat{s} - \hat{m}_\ell^2) \right. \\
& + \frac{1}{4\hat{m}_{K^*}^2} [|B|^2 (\lambda - \hat{u}(\hat{s})^2/3 + 8\hat{m}_{K^*}^2 (\hat{s} + 2\hat{m}_\ell^2)) + |F|^2 (\lambda - \hat{u}(\hat{s})^2/3 + 8\hat{m}_{K^*}^2 (\hat{s} - 4\hat{m}_\ell^2))] \\
& + \frac{\lambda}{\hat{m}_{K^*}^2} [\hat{s}|X|^2 + 2\hat{m}_\ell \lambda (\text{Re}(XF^*) - \hat{s} \text{Re}(XH^*) - (1 - \hat{m}_{K^*}^2) \text{Re}(XG^*))] \\
& + \frac{\lambda}{4\hat{m}_{K^*}^2} [|C|^2 (\lambda - \hat{u}(\hat{s})^2/3) + |G|^2 (\lambda - \hat{u}(\hat{s})^2/3 + 4\hat{m}_\ell^2 (2 + 2\hat{m}_{K^*}^2 - \hat{s}))] \\
& - \frac{1}{2\hat{m}_{K^*}^2} [\text{Re}(BC^* + FG^*) (1 - \hat{m}_{K^*}^2 - \hat{s}) (\lambda - \hat{u}(\hat{s})^2/3) + 4\hat{m}_\ell^2 \text{Re}(FG^*) \lambda] \\
& \left. - 2 \frac{\hat{m}_\ell^2}{\hat{m}_{K^*}^2} \lambda [\text{Re}(FH^*) - \text{Re}(GH^*) (1 - \hat{m}_{K^*}^2)] + |H|^2 \frac{\hat{m}_\ell^2}{\hat{m}_{K^*}^2} \hat{s} \lambda \right\}. \tag{28}
\end{aligned}$$

In the  $B \rightarrow K \ell^+ \ell^-$  case we only need three form factors ( $f_+$ ,  $f_0$  and  $f_T$ ) [54]. Again we define a set of auxiliary variables [50, 51]

$$\begin{aligned}
A' &= C_9^{\text{eff}}(\hat{s}) f_+(\hat{s}) + \frac{2\hat{m}_b}{1 + \hat{m}_K} C_7^{\text{eff}} f_T(\hat{s}), \\
C' &= C_{10}^{\text{eff}} f_+(\hat{s}), \\
D' &= \frac{1 - \hat{m}_K^2}{\hat{s}} C_{10}^{\text{eff}} [f_0(\hat{s}) - f_+(\hat{s})], \\
X' &= \frac{1 - \hat{m}_K^2}{2\hat{m}_b} C_0^\ell f_0(\hat{s}), \tag{29}
\end{aligned}$$

in terms of which

$$\begin{aligned}
\frac{d\Gamma}{d\hat{s}} = & \frac{G_F^2 \alpha_{\text{em}}^2 m_B^5}{2^{10} \pi^5} |V_{tb} V_{ts}^*|^2 \hat{u}(\hat{s}) \left\{ (|A'|^2 + |C'|^2) \left[ \lambda - \frac{\hat{u}(\hat{s})^2}{3} \right] \right. \\
& + 4|C'|^2 \hat{m}_\ell^2 (2 + 2\hat{m}_K^2 - \hat{s}) + 8\text{Re}(C' D'^*) \hat{m}_\ell^2 (1 - \hat{m}_K^2) + 4|D'|^2 \hat{m}_\ell^2 \hat{s} + |X'|^2 (2\hat{s} - 4\hat{m}_\ell^2) \\
& \left. + 4\text{Re}(D' X'^*) \hat{m}_\ell \hat{s} + 4\text{Re}(C' X'^*) \hat{m}_\ell (1 - \hat{m}_K^2) \right\}. \tag{30}
\end{aligned}$$

In comparison to  $B \rightarrow K^{(*)} \ell^+ \ell^-$ , theoretical calculations of the decay amplitudes for  $B \rightarrow K^{(*)} \nu \bar{\nu}$  are considerably more reliable, owing to the absence of long-distance interactions that affect charged-lepton channels. We consider the missing energy distribution of the decay rates in terms of the energy of the neutrino pair in the B rest frame and define the dimensionless variable  $\hat{x} = \hat{E}_{\text{miss}}$ , which varies in the range  $(1 - \hat{m}_{K^{(*)}}^2)/2 < \hat{x} < 1 - \hat{m}_{K^{(*)}}$ . For the  $B \rightarrow K^* \nu \bar{\nu}$  channel,

the partial rate then reads [55, 56]

$$\begin{aligned} \frac{d\Gamma}{d\hat{x}} = & \frac{G_F^2 \alpha_{\text{em}}^2 m_B^5}{128\pi^5} |V_{t,b} V_{t,s}^*|^2 \left| \frac{\delta C_{\nu\bar{\nu}} + X_t}{\sin^2 \theta_W} \right|^2 \lambda^{1/2} \left\{ \hat{s} \left[ (\hat{m}_{K^*} + 1) A_1(\hat{s}) - \frac{\lambda^{1/2} V(\hat{s})}{\hat{m}_{K^*} + 1} \right]^2 \right. \\ & + \hat{s} \left[ (\hat{m}_{K^*} + 1) A_1(\hat{s}) + \frac{\lambda^{1/2} V(\hat{s})}{\hat{m}_{K^*} + 1} \right]^2 \\ & \left. + \left[ \frac{(\hat{m}_{K^*} + 1)^2 \left( \sqrt{\lambda + 4\hat{m}_{K^*}^2} - 2\hat{m}_{K^*}^2 \right) A_1(\hat{s}) - \lambda A_2(\hat{s})}{2\hat{m}_{K^*} (\hat{m}_{K^*} + 1)} \right]^2 \right\}, \end{aligned} \quad (31)$$

while in the case of  $B \rightarrow K \nu \bar{\nu}$  we have

$$\frac{d\Gamma}{d\hat{x}} = \frac{G_F^2 \alpha_{\text{em}}^2 m_B^5}{128\pi^5} |V_{t,b} V_{t,s}^*|^2 \left| \frac{\delta C_{\nu\bar{\nu}} + X_t}{\sin^2 \theta_W} \right|^2 f_+(\hat{s}) \lambda^{3/2}. \quad (32)$$

### 3.3 $B \rightarrow X_s \gamma$

Since the scalar-density operator does not contribute to  $B \rightarrow X_s \gamma$ , in this case the treatment is completely equivalent to the SM. We can thus take advantage of the complete NNLO analysis of Ref. [11]. Expressing the branching ratio in terms of the initial conditions of  $C_7$  and expanding around the SM value we can write [11, 12, 57]

$$\mathcal{B}(B \rightarrow X_s \gamma)_{[E_\gamma > 1.6 \text{ GeV}]} = \left| \frac{V_{ts} V_{tb}^*}{V_{cb}} \right|^2 \frac{6.00 \times 10^{-5}}{C_{uc}} [3.15 - 7.18 \delta C_7 + 4.74 (\delta C_7)^2]. \quad (33)$$

where  $C_{uc} = |V_{ub}/V_{cb}|^2 \Gamma(B \rightarrow X_c e \nu) / \Gamma(B \rightarrow X_u e \nu)$  and its numerical value is reported in Table 3. Following Ref. [11] we assign a theoretical error of  $0.23 \times 10^{-4}$  to this expression.

Thanks to the precise experimental measurement of the  $B \rightarrow X_s \gamma$  rate, Eq. (33) provide a very stringent bound on non-standard contributions to electric-dipole and chromomagnetic operators. As anticipated, we do not treat  $\delta C_8$  as an independent parameter in the fit: the bounds on  $\delta C_7$  derived by means of Eq. (33) should be interpreted as bounds on the linear  $\delta C_7$ – $\delta C_8$  combination in Eq. (11).

### 3.4 $B_{s,d} \rightarrow \ell^+ \ell^-$

The pure leptonic decays  $B_s \rightarrow \ell^+ \ell^-$  receive contributions only from the effective operators  $P_{10}$  and  $P_0^\ell$ . These are free from the contamination of four-quark operators, which makes the generalization to the  $b \rightarrow d$  case straightforward.

The  $B_s \rightarrow \ell^+ \ell^-$  rates can be written as

$$\Gamma(B_s \rightarrow \ell^+ \ell^-) = \frac{\alpha_{\text{em}}^2 G_F^2 |V_{tb}^* V_{ts} A_{10}|^2}{16\pi^3} m_{B_s} m_\ell^2 f_{B_s}^2 \sqrt{1 - 4 \frac{m_\ell^2}{m_{B_s}^2}} \left[ |1 + \delta_S|^2 + \left( 1 - 4 \frac{m_\ell^2}{m_{B_s}^2} \right) |\delta_S|^2 \right], \quad (34)$$

where

$$\delta_S = \frac{C_0^\ell m_{B_s}^2}{4A_{10}(m_b + m_s)m_\ell} = \frac{C_0^\ell}{\lambda_\ell \lambda_b} \frac{m_{B_s}^2 \tan \beta^2}{4A_{10} \langle H_U \rangle^2} \frac{m_b}{m_b + m_s}. \quad (35)$$

Quantity	Value
$ V_{us} $	$0.2255 \pm 0.0007$ [33]
$ V_{cb} $	$(4.1 \pm 0.1) \times 10^{-2}$ [10]
$ V_{ub} $	$(3.8 \pm 0.4) \times 10^{-3}$ [10]
$\gamma$	$(70.3 \pm 6.3)^o$ [9]
$f_{B_s}$	$(0.260 \pm 0.030)$ GeV [26]
$f_{B_s}/f_{B_d}$	$(1.21 \pm 0.06)$ [59]
$\mathcal{B}(B \rightarrow X_c \ell \nu)$	$(10.75 \pm 0.16) \times 10^{-2}$ [10]
$C_{uc}$	$0.58 \pm 0.01$ [11]

Table 3: Main inputs used in the numerical analysis (inputs not explicitly indicated in this Table are taken from Ref. [58]).

The  $B_d \rightarrow \ell^+ \ell^-$  rates are obtained from Eq. (34) with the exchange  $\{V_{ts}, m_{B_s}, m_s\} \rightarrow \{V_{td}, m_{B_d}, m_d\}$ . Neglecting tiny corrections of  $O(m_s/m_b)$ , this leads to one of the most stringent tests of the MFV scenario, both at small and large  $\tan \beta$  values, namely the relation

$$\frac{\Gamma(B_s \rightarrow \ell^+ \ell^-)}{\Gamma(B_d \rightarrow \ell^+ \ell^-)} \approx \frac{f_{B_s} m_{B_s}}{f_{B_d} m_{B_d}} \left| \frac{V_{ts}}{V_{td}} \right|^2. \quad (36)$$

On the other hand, we stress that the relation between  $B_{s,d} \rightarrow \ell^+ \ell^-$  rates and  $\Delta F = 2$  observables discussed in [38] holds only in specific (constrained) versions of the MFV scenario.

### 3.5 $K \rightarrow \pi \nu \bar{\nu}$

The branching ratio of charged and neutral  $K \rightarrow \pi \nu \bar{\nu}$  decays can be simply expressed as

$$\mathcal{B}(K^+ \rightarrow \pi^+ \nu \bar{\nu}) = \kappa_\nu^+ (1 + \Delta_{EM}) |y_\nu|^2, \quad \mathcal{B}(K_L \rightarrow \pi^0 \nu \bar{\nu}) = \kappa_\nu^L [Im(y_\nu)]^2, \quad (37)$$

where from [33, 37]  $\kappa_\nu^+ = 0.7867(43) \times 10^{-5}$  and  $\kappa_\nu^L = 3.3624(264) \times 10^{-5}$  whereas the electromagnetic corrections  $\Delta_{EM} = -(0.30 \pm 0.05)\%$ . Similarly to  $B_{s,d} \rightarrow \ell^+ \ell^-$  rates, also in this case we have two observables controlled by a single free parameter: the real coefficient  $\delta C_{\nu \bar{\nu}}$  in Eq. (20). Thus also in this case the ratio of the two  $K \rightarrow \pi \nu \bar{\nu}$  rates leads to a significant model-independent test of the MFV hypothesis.

## 4 Numerical analysis

In order to determine the presently allowed range of the  $\delta C_i$  we have performed a global fit of the  $\Delta F = 1$  observables in Table 1. The main numerical inputs beside rare processes used in the fits are reported in Table 3. The latter have been assumed to be not correlated and not polluted by new physics effects. In particular, as far the CKM angle  $\gamma$  is concerned, we have used the results of Ref. [9] where the CKM matrix is determined using only tree-level observables. Our fitting procedure follows the method adopted by the UTFit collaboration [9]: we integrate over the probability distributions of inputs and conditional probability distributions of observables assuming validity of MFV to obtain (after proper normalization) the probability distributions for the  $\delta C_i$ .

The resulting ranges for the  $\delta C_i$  and the corresponding bounds on the scale of new physics for the various operators are shown in Tables 4 and 5, and in Fig. 1. The bounds in Table 4 are the

$\delta C_i$	95% probability bound	Observables
$\delta C_7$	$[-0.14, 0.06] \cup [1.42, 1.62]$	$B \rightarrow X_s \gamma, B \rightarrow X_s \ell^+ \ell^-$
$\delta C_9$	$[-2.8, 0.8]$	$B \rightarrow X_s \ell^+ \ell^-$
$\delta C_{10}$	$[-0.4, 2.3]$	$B \rightarrow X_s \ell^+ \ell^-, B_s \rightarrow \mu^+ \mu^-$
$\delta C_S^\mu / m_b$	$[-0.09, 0.09] / (4.2 \text{ GeV})$	$B_s \rightarrow \mu^+ \mu^-$
$\delta C_{\nu\bar{\nu}}$	$[-6.1, 2.0]$	$K^+ \rightarrow \pi^+ \nu \bar{\nu}$

Table 4: Combined bounds on the effective Wilson coefficients in the MFV scenario, and observables used to derive the bounds (in the case of the scalar operator we report the bound in terms of the scale-independent combination  $\delta C_S^\mu / m_b$ ).

Operator	$\Lambda_i @ 95\% \text{ prob. [TeV]}$	Observables
$H_D^\dagger (\bar{D}_R \lambda_d \lambda_{\text{FC}} \sigma_{\mu\nu} Q_L) (e F_{\mu\nu})$	6.1	$B \rightarrow X_s \gamma, B \rightarrow X_s \ell^+ \ell^-$
$H_D^\dagger (\bar{D}_R \lambda_d \lambda_{\text{FC}} \sigma_{\mu\nu} T^a Q_L) (g_s G_{\mu\nu}^a)$	3.4	$B \rightarrow X_s \gamma, B \rightarrow X_s \ell^+ \ell^-$
$(\bar{Q}_L \lambda_{\text{FC}} \gamma_\mu Q_L) (e D_\mu F_{\mu\nu})$	1.5	$B \rightarrow X_s \ell^+ \ell^-$
$i (\bar{Q}_L \lambda_{\text{FC}} \gamma_\mu Q_L) H_U^\dagger D_\mu H_U$	1.1 <sup>a</sup>	$B \rightarrow X_s \ell^+ \ell^-, B_s \rightarrow \mu^+ \mu^-$
$i (\bar{Q}_L \lambda_{\text{FC}} \tau^a \gamma_\mu Q_L) H_U^\dagger \tau^a D_\mu H_U$	1.1 <sup>a</sup>	$B \rightarrow X_s \ell^+ \ell^-, B_s \rightarrow \mu^+ \mu^-$
$(\bar{Q}_L \lambda_{\text{FC}} \gamma_\mu Q_L) (\bar{L}_L \gamma_\mu L_L)$	1.7	$B \rightarrow X_s \ell^+ \ell^-, B_s \rightarrow \mu^+ \mu^-$
$(\bar{Q}_L \lambda_{\text{FC}} \gamma_\mu \tau^a Q_L) (\bar{L}_L \gamma_\mu \tau^a L_L)$	1.7	$B \rightarrow X_s \ell^+ \ell^-, B_s \rightarrow \mu^+ \mu^-$
$(\bar{Q}_L \lambda_{\text{FC}} \gamma_\mu Q_L) (\bar{E}_R \gamma_\mu E_R)$	2.7	$B \rightarrow X_s \ell^+ \ell^-, B_s \rightarrow \mu^+ \mu^-$

<sup>a</sup>A discrete ambiguity is removed at 90% probability, improving the bound to 2.3 TeV.

Table 5: Individual bounds on the scale of new physics for the most relevant MFV operators.

results of the global fit, where all the  $\delta C_i$  are allowed to vary. The most interesting correlations among pairs of  $\delta C_i$  of the global fit are shown in Fig. 1. On the other hand, the bounds in Table 5 correspond to the bound on the scale of each non-standard operator, assuming the others to have a negligible impact. Note that the correlations of the  $\delta C_i$  play a non-trivial role also in Table 5, by means of Eq. (6): each bound corresponds to setting one of the  $a_i = \pm 1$  and the others to zero. In case of sign ambiguities, the bound on the scale corresponds to the lower allowed value.

In the case of the scalar-density operator, the translation of the bound on  $\delta C_S^\mu$  into a bound on the scale is not straightforward as for the other operators. Assuming that the coefficient of  $\mathcal{O}_{S1}$  in Eq. (1) does not depend on  $\tan \beta$  and setting  $a_{S1} = \pm 1$  we get

$$\Lambda_{[\mathcal{O}_{S1}]} > \Lambda_0 \left( \frac{\lambda_b \lambda_\mu}{|\delta C_S^\mu|_{\text{max}}} \right)^{1/2} = (1.5 \text{ TeV}) \times \left( \frac{\tan \beta}{50} \right) [95\% \text{ prob.}] . \quad (38)$$

This bound, comparable to most of the bounds in Table 5, is especially interesting in specific models, where it can be identified with a bound on the mass of heavy Higgs fields. This happens for instance in the MSSM, where  $a_{S1}$  is suppressed by  $1/16\pi^2$  ( $\mathcal{O}_{S1}$  being forbidden at the tree level by the Peccei-Quinn symmetry) but grows linearly with  $\tan \beta$  [1]. In particular, setting  $|a_{S1}|/\Lambda^2 = \tan \beta / (16\pi^2 M_H^2)$ , leads to

$$M_H > (830 \text{ GeV}) \times \left( \frac{\tan \beta}{50} \right)^{3/2} [95\% \text{ prob.}] . \quad (39)$$

As far the sign of  $C_7$  is concerned, we find that the *wrong sign* solution to  $C_7$  is still allowed, but has a lower probability compared to the SM sign. As shown in Fig. 2, the large contribution

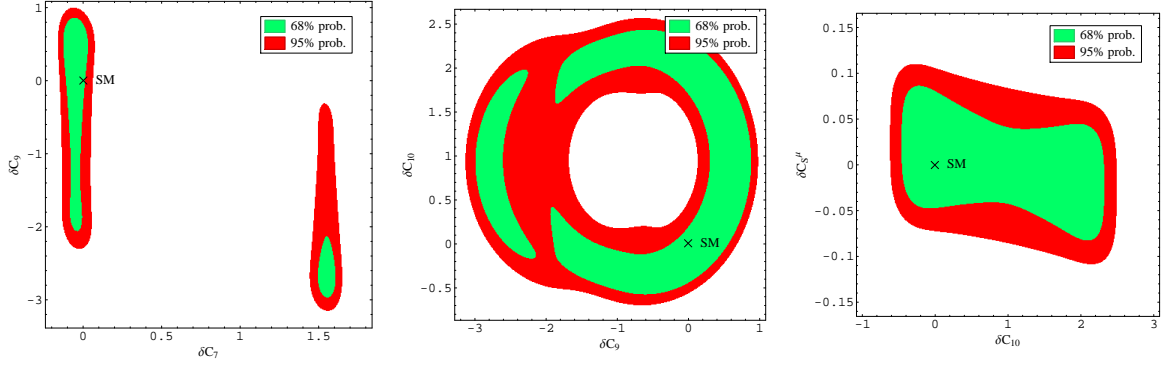


Figure 1: Correlation plots for the pairs of shifts in the Wilson coefficients. Allowed regions at 68% (in green) and 95% (in red) probability.

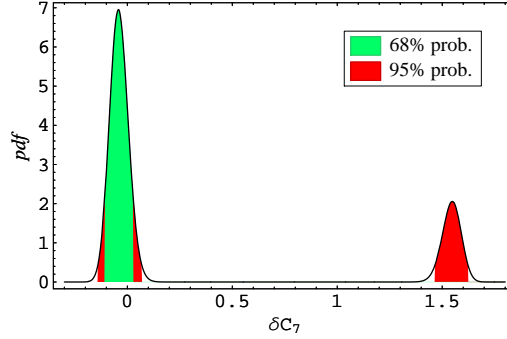


Figure 2: Probability distribution of  $\delta C_7$ .

to  $\delta C_7$ , corresponding to a sign flip of  $C_7(m_b)$ , has a probability of about 30%. We stress that the sign flip of  $C_7(m_b)$  occurs only if  $C_9$  receives a sizable non-standard contribution. This is consistent with the conclusion of Ref. [60], where the wrong sign solution to  $C_7$  has been excluded assuming small new-physics effects in the other Wilson coefficients.

The impact of the low- and high-energy regions in  $B \rightarrow X_s \ell^+ \ell^-$ , which are often neglected, can be seen in Fig. 3, where we plot the most interesting 68% and 95% allowed regions with or without the information of these two measurements. In view of future experimental improvements, we report below the numerical values of the main observables expanded in powers of the  $\delta C_i$ :

$$\mathcal{B}(B \rightarrow X_s \gamma)(E_\gamma > 1.6 \text{ GeV}) = 3.13(23) \times 10^{-4} \times (1 - 2.28\delta C_7 + 1.51\delta C_7^2), \quad (40)$$

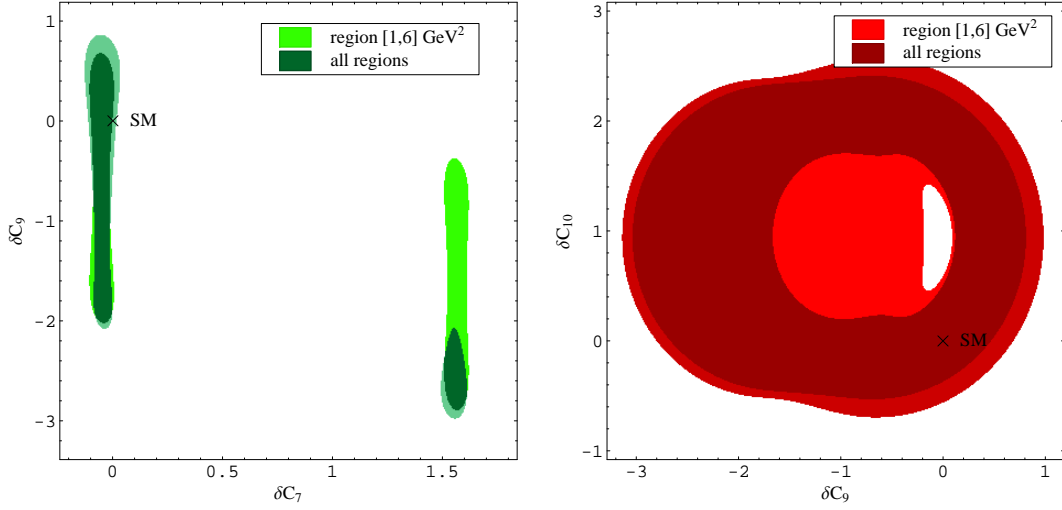


Figure 3: Correlation plots for the pairs of shifts in the Wilson coefficients, which are most affected by including the low and high energy regions in  $B \rightarrow X_s \ell^+ \ell^-$ . The left plot shows regions allowed at 68% (in green) while in the right plot, the regions shown are allowed at 95% (in red). The dark and light shaded regions correspond to the fit with and without the low and high energy regions in  $B \rightarrow X_s \ell^+ \ell^-$  respectively.

$$\begin{aligned}
\mathcal{B}(B \rightarrow X_s \ell^+ \ell^-)(q^2 \in [0.0021, 0.04] \text{ GeV}^2) &= 0.8(2) \times 10^{-6} \\
&\times [1 + 2.02\delta C_7^2 + 0.20\delta C_9^2 + 0.20\delta C_{10}^2 - 2.23\delta C_7 + 0.23\delta C_9 - 0.37\delta C_{10} + 0.31\delta C_7\delta C_9 \\
&+ 0.01(\delta C_S^\mu)^2 - 0.01\delta C_{10}\delta C_S^\mu + 0.01\delta C_S^\mu] \\
\mathcal{B}(B \rightarrow X_s \ell^+ \ell^-)(q^2 \in [1.0, 6.0] \text{ GeV}^2) &= 1.6(1) \times 10^{-6} \\
&\times [1 + 0.64\delta C_7^2 + 0.61\delta C_9^2 + 0.61\delta C_{10}^2 - 0.03\delta C_7 + 0.86\delta C_9 - 1.15\delta C_{10} + 0.73\delta C_7\delta C_9 \\
&+ 0.13(\delta C_S^\mu)^2 - 0.03\delta C_{10}\delta C_S^\mu + 0.04\delta C_S^\mu] , \\
\mathcal{B}(B \rightarrow X_s \ell^+ \ell^-)(q^2 \in [14.4, 25.0] \text{ GeV}^2) &= 2.3(7) \times 10^{-7} \\
&\times [1 + 0.05\delta C_7^2 + 0.28\delta C_7 + 0.59\delta C_9^2 + 0.59\delta C_{10}^2 + 1.04\delta C_9 - 1.13\delta C_{10} + 0.32\delta C_7\delta C_9 \\
&+ 0.27(\delta C_S^\mu)^2 - 0.02\delta C_{10}\delta C_S^\mu + 0.02\delta C_S^\mu] , \tag{41}
\end{aligned}$$

$$\mathcal{B}(B_s \rightarrow \mu^+ \mu^-) = 4.1(8) \times 10^{-9} \times [(1 - 1.04\delta C_{10} - 29.3\delta C_S^\mu)^2 + 860(\delta C_S^\mu)^2] , \tag{42}$$

$$\mathcal{B}(K^+ \rightarrow \pi^+ \nu \bar{\nu}) = 8.6(9) \times 10^{-11} [1 + 0.96\delta C_{\nu\bar{\nu}} + 0.24\delta C_{\nu\bar{\nu}}^2] . \tag{43}$$

Since the experimental information of exclusive  $B \rightarrow K^* \ell^+ \ell^-$  modes is quite good [27], we have also investigated the impact of including these observables in the fit. In this case we have used the results of Ref. [31] for the hadronic form factors and their corresponding errors, taking into account additional theoretical uncertainty due to neglected additional long distance effects [28–30].

The FB asymmetry plays a significant role. In particular, the normalised FB asymmetry

$$\bar{\mathcal{A}}_{\text{FB}}(q^2) = \frac{1}{d\Gamma/dq^2} \frac{d\mathcal{A}_{\text{FB}}}{dq^2} \tag{44}$$

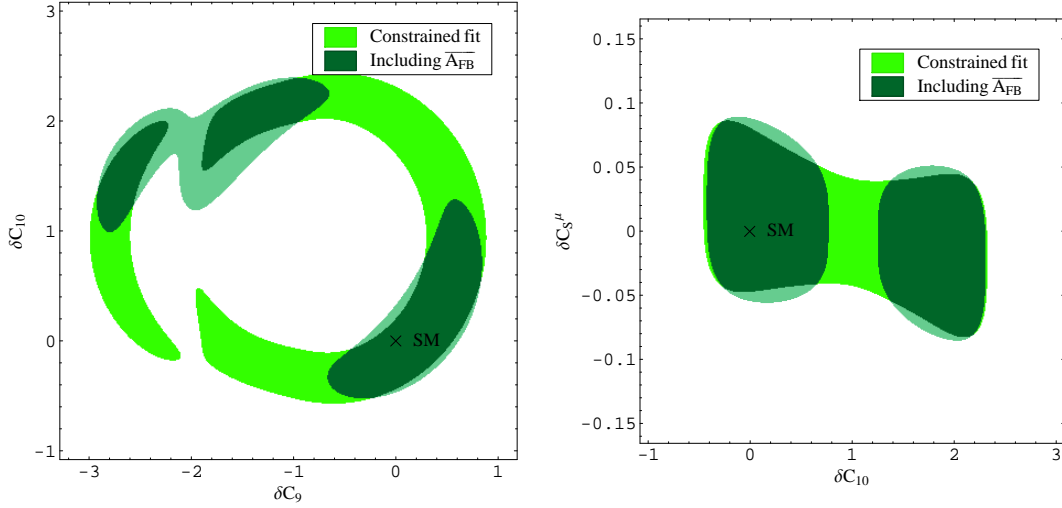


Figure 4: Correlation plots for the pairs of shifts in the Wilson coefficients, which are most affected by including the exclusive  $A_{FB}$  observables. Allowed regions at 68% with (dark green) and without (light green) exclusive  $A_{FB}$  observables are shown.

is interesting since the main uncertainty due to the form factors, namely the overall normalization of the decay rate, partly cancels out. Moreover,  $A_{FB}(B \rightarrow K^* \ell^+ \ell^-)$  in the low  $q^2$  energy region is very small in the SM due to the destructive interference of  $C_7$  and  $C_9$  (resulting in the famous zero of the asymmetry at low  $q^2$ ). It is therefore a good probe of the relative sign of the Wilson coefficients. The impact of including the presently available data on  $A_{FB}(B \rightarrow K^* \ell^+ \ell^-)$  is shown in Fig. 4.<sup>5</sup> As can be seen, at present the additional information significantly reduces part of the ambiguities in the  $\delta C_9$ – $\delta C_{10}$  and  $\delta C_{10}$ – $\delta C_0^\mu$  planes only at 68% probability level. On the other hand, the overall bounds on the scales of individual coefficients do not change in appreciable way. This may seem at odds with conclusions reached in refs. [27, 61]. However, the central experimental values for the high  $q^2$  region lie approximately 1.5 standard deviations above the range of possible theory predictions within MFV satisfying other bounds. In addition, this range of theory predictions spans less than two experimental standard deviations. Under the assumption of MFV validity, the present FB asymmetry measurements therefore cannot significantly affect the 95% probability regions of  $\delta C_i$ . As seen on Fig. 4, the situation would however improve dramatically, once the experimental precision would approximately double.

Contrary to the FB asymmetry, it turns out that the  $K^*$  longitudinal polarization is not very sensitive to new physics in the MFV scenario.

For completeness, we report below the numerical expressions of  $A_{FB}(B \rightarrow K^* \ell^+ \ell^-)$ , integrated

<sup>5</sup>  $A_{FB}(B \rightarrow K^* \ell^+ \ell^-)$  has been measured both by Belle [61] and Babar [27]. However, in Ref. [61] only the fully integrated asymmetry has been reported. The normalised values of  $A_{FB}(B \rightarrow K^* \ell^+ \ell^-)$  in different  $q^2$  bins, as reported in Ref. [27], represent the most useful information for our purpose. For this reason, we have restricted our numerical analysis only to the results in Ref. [27].



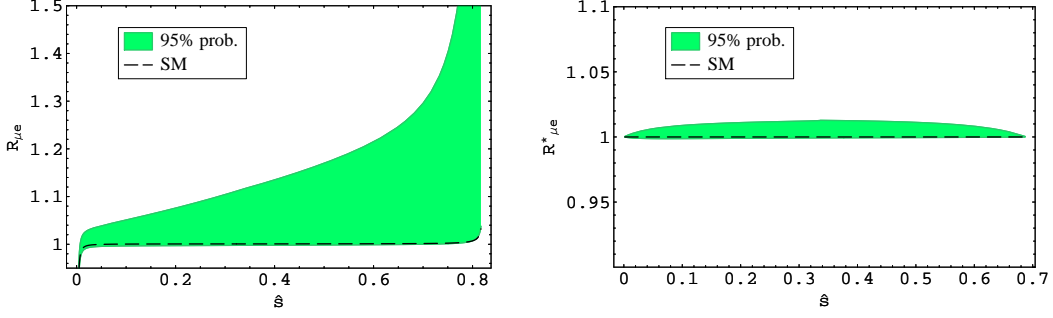


Figure 5: 95% probability allowed ranges for the lepton universality ratio (muon/electron) for the differential distributions of  $B \rightarrow K \ell^+ \ell^-$  (left) and  $B \rightarrow K^* \ell^+ \ell^-$  (right).

and normalised to the decay rate as in Ref. [27] expanded in powers of the  $\delta C_i$ :

$$\begin{aligned}
\frac{\mathcal{A}_{\text{FB}}(B \rightarrow K^* \ell^+ \ell^-)_{q^2 < 6.25 \text{ GeV}^2}}{\Gamma(B \rightarrow K^* \ell^+ \ell^-)_{q^2 < 6.25 \text{ GeV}^2}} &= -0.01(2) \times \\
&\times \frac{(1 - 20\delta C_7 - 11\delta C_9 + 1\delta C_{10} + 21\delta C_7\delta C_{10} + 11\delta C_9\delta C_{10})}{(1 + 1.2\delta C_7^2 - 0.7\delta C_7 + 0.5\delta C_9^2 + 0.5\delta C_{10}^2 + 0.6\delta C_9 - 1.0\delta C_{10} + 0.8\delta C_7\delta C_9)}, \\
\frac{\mathcal{A}_{\text{FB}}(B \rightarrow K^* \ell^+ \ell^-)_{q^2 > 10.24 \text{ GeV}^2}}{\Gamma(B \rightarrow K^* \ell^+ \ell^-)_{q^2 > 10.24 \text{ GeV}^2}} &= 0.20(8) \times \\
&\times \frac{(1 + 0.5\delta C_7 + 1.2\delta C_9 - 1.0\delta C_{10} - 0.5\delta C_7\delta C_{10} - 1.3\delta C_9\delta C_{10})}{(1 + 0.1\delta C_7^2 + 0.4\delta C_7 + 0.6\delta C_9^2 + 0.6\delta C_{10}^2 + 1.0\delta C_9 - 1.2\delta C_{10} + 0.4\delta C_7\delta C_9)}. \quad (45)
\end{aligned}$$

In the above expressions, we have neglected the scalar operator contributions, which are made negligible by the strong bound coming from  $B_s \rightarrow \mu^+ \mu^-$ . However,  $\delta C_S^\mu$  dominates possible NP effects in the lepton universality ratios of  $B \rightarrow K^{(*)} \ell^+ \ell^-$ , as we discuss in the next section.

## 5 Predictions

Using the bounds on the MFV operators discussed in the previous section, we obtain a series of constraints for FCNC processes which are not well measured yet. The most interesting predictions can be summarised as follows:

- $R^{(\mu/e)}(B \rightarrow K^{(*)} \ell^+ \ell^-)$ .

As pointed out in Ref. [51] the lepton universality ratios (or the muon to electron ratios of branching ratios) in  $B \rightarrow K^{(*)} \ell^+ \ell^-$  are very clean probes of possible scalar density operators. Within the MFV framework there is a one-to-one correspondence between possible deviations from the SM in the lepton universality ratios and the contribution of the scalar-density operator in  $B_s \rightarrow \mu^+ \mu^-$ . Thanks to the substantial improvement on  $B_s \rightarrow \mu^+ \mu^-$ , the effect is highly constrained.

The present allowed ranges for the differential distributions of the lepton universality ratios are shown in Fig. 5. As can be seen, the effect is negligibly small in the  $B \rightarrow K^*$  case. In the  $B \rightarrow K$  case there is still some room for deviations from the SM, but only in the high- $q^2$  region, where the decay is suppressed. The maximal integrated effect is reported in Table 6.

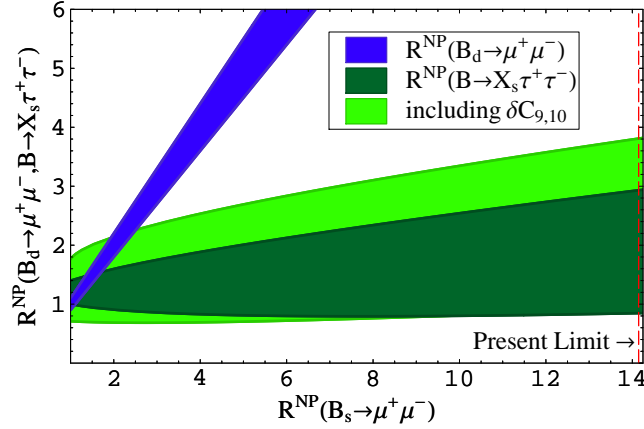


Figure 6: Correlations between  $B_s \rightarrow \mu^+\mu^-$ ,  $B_d \rightarrow \mu^+\mu^-$ , and  $B_s \rightarrow X_s\tau^+\tau^-$ . For a given value of  $\mathcal{B}(B_s \rightarrow \mu^+\mu^-)$ , normalised to the SM prediction (horizontal axis), we plot the range of  $\mathcal{B}(B_d \rightarrow \mu^+\mu^-)$  and  $\mathcal{B}(B_s \rightarrow X_s\mu^+\mu^-)$ , both normalised to the corresponding SM predictions (vertical axis).

Note the major improvement with respect to the analysis of Ref. [51], where the loose bound on  $B_s \rightarrow \mu^+\mu^-$  allowed much larger non-standard effects.

- $\mathcal{B}(B_d \rightarrow \mu^+\mu^-)$

As anticipated, probably the best test of the MFV scenario in the  $\Delta F = 1$  sector is the ratio in Eq. (36). Taking into account the present bound on  $B_s \rightarrow \mu^+\mu^-$  this implies the upper limit

$$\mathcal{B}(B_d \rightarrow \mu^+\mu^-) < 1.2 \times 10^{-9}, \quad (46)$$

at 95% probability. The clear correlation between  $\mathcal{B}(B_d \rightarrow \mu^+\mu^-)$  and  $\mathcal{B}(B_s \rightarrow \mu^+\mu^-)$  in the MFV framework is illustrated in Fig. 6.

- $\mathcal{B}(B \rightarrow X_s\tau^+\tau^-)$

The bound on the scalar-current operator allows us to derive a non-trivial bound also on  $\mathcal{B}(B \rightarrow X_s\tau^+\tau^-)$ , which at large  $\tan\beta$  is sensitive to scalar-current operators. The parametrical dependence on the modified Wilson coefficient of the integrated branching ratio is

$$\begin{aligned} \mathcal{B}(B \rightarrow X_s\tau^+\tau^-)_{q^2 \in [14.4, 25.0] \text{ GeV}^2} &= 1.6(5) \times 10^{-7} \\ &\times (1 + 0.06\delta C_7^2 + 0.38\delta C_7 + 0.81\delta C_9^2 + 0.41\delta C_{10}^2 + 1.41\delta C_9 \\ &- 0.78\delta C_{10} + 0.43\delta C_7\delta C_9 - 0.54\delta C_{10}\delta C_S^\tau + 0.52\delta C_S^\tau + 0.32\delta C_S^{\tau 2}). \end{aligned} \quad (47)$$

Assuming  $\delta C_S^\tau = (m_\tau/m_\mu)\delta C_S^\mu$ , in agreement with Eq. (6), and taking into account the allowed ranges of the Wilson coefficients in Table 4, we obtain the 95% probability bound reported in Table 6.

- $dA_{FB}/dq^2(B \rightarrow X_s\ell^+\ell^-)$

Taking into account the available constraints on  $C_{7,9,10}$ , the resulting allowed range for the inclusive FB asymmetry is shown in Fig. 7. As can be seen, in this case there is still a large room for non-standard effects: this observable is one of the few examples of quantities which

Observable	Experiment	MFV bound	SM prediction
$R^{(\mu/e)}(B \rightarrow K\ell^+\ell^-) - 1$	$0.17 \pm 0.28$ [62, 63] <sup>a</sup>	$[-0.004, 0.14]$	$O(10^{-4})$ [64]
$R^{(\mu/e)}(B \rightarrow K^*\ell^+\ell^-) - 1$	$0.37_{-0.40}^{+0.53} \pm 0.09$ [63]	$[-0.002, 0.01]$	$\lesssim 10^{-2}$
$\mathcal{B}(B_d \rightarrow \mu^+\mu^-)$	$< 1.8 \times 10^{-8}$ [24]	$< 1.2 \times 10^{-9}$	$1.3(3) \times 10^{-10}$
$\mathcal{B}(B \rightarrow X_s\tau^+\tau^-)$	–	$< 5 \times 10^{-7}$	$1.6(5) \times 10^{-7}$
$\mathcal{B}(B \rightarrow K\nu\bar{\nu})$	[65]	$< 0.4 \times 10^{-4}$	$(0.5 \pm 0.1) \times 10^{-5}$
$\mathcal{B}(B \rightarrow K^*\nu\bar{\nu})$	[65]	$< 9.4 \times 10^{-5}$	$(1.2 \pm 0.3) \times 10^{-5}$
$\mathcal{B}(K_L \rightarrow \pi^0\nu\bar{\nu})$	[66]	$< 2.9 \times 10^{-10}$	$2.9(5) \times 10^{-11}$

<sup>a</sup>Here we quote naïve averages of the values obtained by the experiments and with symmetrized errors.

Table 6: Predicted observables. All bounds are 95% probability limits. In the first two lines, the SM predictions refer to the kinematical region where lepton-mass phase-space effects can be safely neglected. The experimental results on  $\nu\bar{\nu}$  modes are not explicitly indicated since only 90% C.L. limits are available.

could exhibit large deviations from the SM even in the pessimistic MFV framework. On the other hand, present data exclude most configurations with flipped  $\text{sgn}(C_9/C_{10})$  at 68% probability.

- $\mathcal{B}(B \rightarrow K^{(*)}\nu\bar{\nu})$  and  $\mathcal{B}(K_L \rightarrow \pi^0\nu\bar{\nu})$

From the  $K^+ \rightarrow \nu\bar{\nu}$  bound on  $\delta C_{\nu\nu}$  we can bound the rates of all the  $\nu\bar{\nu}$ -type FCNC transitions<sup>6</sup>. The most interesting predictions are reported in Table 6 (in the  $\mathcal{B}(B \rightarrow K^{(*)}\nu\bar{\nu})$  case we take into account form-factor uncertainties along the lines discussed in Section 3.2). For completeness, we give the numerical expressions of the  $K_L \rightarrow \pi^0\nu\bar{\nu}$  and  $B \rightarrow K^{(*)}\nu\bar{\nu}$  branching ratios:

$$\begin{aligned}
\mathcal{B}(K_L \rightarrow \pi^0\nu\bar{\nu}) &= 2.9(5) \times 10^{-11} [1 + 1.37\delta C_{\nu\bar{\nu}} + 0.47\delta C_{\nu\bar{\nu}}^2] , \\
\mathcal{B}(B \rightarrow K\nu\bar{\nu}) &= 0.5(1) \times 10^{-5} [1 + 1.2\delta C_{\nu\bar{\nu}} + 0.4\delta C_{\nu\bar{\nu}}^2] , \\
\mathcal{B}(B \rightarrow K^*\nu\bar{\nu}) &= 1.2(3) \times 10^{-5} [1 + 1.2\delta C_{\nu\bar{\nu}} + 0.4\delta C_{\nu\bar{\nu}}^2] .
\end{aligned} \tag{48}$$

## 6 Conclusions

The MFV hypothesis provides an efficient tool to analyse flavour-violating effects in extensions of the SM. The effective theory built on this symmetry and and symmetry-breaking hypothesis leads to: 1) a natural suppression of flavour violating effects, in agreement with present observations, even for new physics in the TeV range; 2) a series of experimentally testable predictions, which could help to identify the underlying mechanism of flavour symmetry breaking.

In this paper we have presented a general analysis of the MFV effective theory in the  $\Delta F = 1$  sector. From the current stringent bounds on possible deviations from the SM in various  $B$ -physics observables we have derived the bounds on the scale of new-physics reported in Table 5. As can be seen, these bounds are perfectly compatible with new dynamics in the TeV range. We recall that in models where new particles contribute to FCNC processes only at the loop level, the bounds on the particle masses are one order of magnitude weaker with respect to the bounds reported

<sup>6</sup>These predictions are valid only in the limit where we can neglect operators with the  $Y_u^\dagger Y_u Y_d^\dagger Y_d$  flavour structure. This condition is always fulfilled at small/moderate  $\tan\beta$  and even at large  $\tan\beta$  holds in most explicit MFV scenarios.

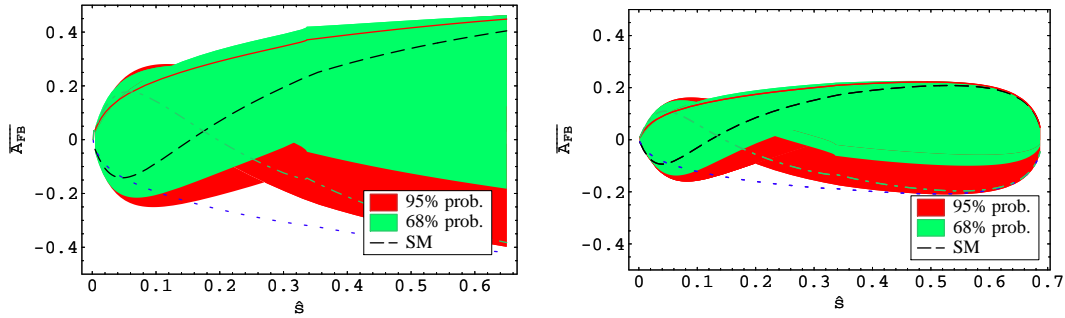


Figure 7: 95% probability allowed range for the inclusive normalised FB asymmetry in  $B \rightarrow X_s \ell^+ \ell^-$  (left) and  $B \rightarrow K^* \ell^+ \ell^-$  (right). The dashed curve denotes the central value of the SM prediction. The other three lines indicate the central values obtained flipping  $\text{sgn}(C_7/C_{10})$  and/or  $\text{sgn}(C_9/C_{10})$ .

in Table 5:  $\Lambda \sim 4\pi m_{\text{NP}}$ . Thus in weakly-interacting theories respecting the MFV hypothesis and with no tree-level FCNC, we could expect new particles well within the reach of the LHC.

Using the bounds on the effective operators, taking into account the correlations implied by the observables measured so far, we have derived a series of predictions for future high-statistics studies of flavour physics. This has allowed us to identify observables which could still exhibit large deviations for the SM even under the pessimistic hypothesis of MFV. The most interesting ones are the rare decays  $B_{s,d} \rightarrow \mu^+ \mu^-$ , rare  $B$  and  $K$  decays with a neutrino pair in the final state, and the FB asymmetry in  $B \rightarrow K^* \ell^+ \ell^-$  decays. The allowed parameter space for the latter is shown in Fig. 7.

Using the current bounds on MFV operators we have also identified a series of stringent tests of this symmetry principle. The most interesting *negative predictions* are summarised in Table 6. If these predictions were falsified by future experiments, we could unambiguously conclude that there exist new flavour symmetry-breaking structures beyond the SM Yukawa couplings. The effective theory allows us to obtain also some *positive predictions*, namely correlations among different observables which could still exhibit a deviation from the SM. The most interesting of such positive predictions is the correlation between  $B_s \rightarrow \mu^+ \mu^-$  and  $B_d \rightarrow \mu^+ \mu^-$  implied by Eq. (36) and illustrated in Fig. 6. A clear evidence of physics beyond the SM in both channels, respecting this correlation, would provide a strong support of the MFV hypothesis.

## Acknowledgements

We thank J. Charles, S. Descotes-Genon and U. Haisch for interesting discussions, and D. Guadagnoli for his comments on the manuscript. This work is supported by the EU under contract MTRN-CT-2006-035482 *Flavianet*.

## References

- [1] G. D'Ambrosio, G. F. Giudice, G. Isidori and A. Strumia, Nucl. Phys. B **645** (2002) 155 [arXiv:hep-ph/0207036].
- [2] R. S. Chivukula and H. Georgi, Phys. Lett. B **188** (1987) 99.

- [3] A. J. Buras, *et al.* Phys. Lett. B **500** (2001) 161 [arXiv:hep-ph/0007085].
- [4] A. Ali and D. London, Eur. Phys. J. C **9** (1999) 687 [arXiv:hep-ph/9903535]; A. J. Buras, Acta Phys. Polon. B **34** (2003) 5615 [arXiv:hep-ph/0310208]; B. Grinstein, V. Cirigliano, G. Isidori and M. B. Wise, Nucl. Phys. B **763** (2007) 35 [arXiv:hep-ph/0608123].
- [5] E. Gabrielli and G. F. Giudice, Nucl. Phys. B **433**, 3 (1995) [Erratum-ibid. B **507**, 549 (1997)] [arXiv:hep-lat/9407029]; L. J. Hall and L. Randall, Phys. Rev. Lett. **65** (1990) 2939.
- [6] P. Paradisi, M. Ratz, R. Schieren and C. Simonetto, arXiv:0805.3989 [hep-ph]; G. Colangelo, E. Nikolidakis and C. Smith, arXiv:0807.0801 [hep-ph]; B. Dudley and C. Kolda, arXiv:0805.4565 [hep-ph].
- [7] E. Nikolidakis and C. Smith, Phys. Rev. D **77**, 015021 (2008) [arXiv:0710.3129 [hep-ph]].
- [8] G. Cacciapaglia, C. Csaki, J. Galloway, G. Marandella, J. Terning and A. Weiler, JHEP **0804** (2008) 006 [arXiv:0709.1714 [hep-ph]].
- [9] M. Bona *et al.* [UTfit Collaboration], JHEP **0803** (2008) 049 [arXiv:0707.0636 [hep-ph]]; for UT angle  $\gamma$  we use the updated value on <http://www.utfit.org/>.
- [10] E. Barberio *et al.* [Heavy Flavor Averaging Group (HFAG) Collaboration], arXiv:0704.3575 [hep-ex], and online update at <http://www.slac.stanford.edu/xorg/hfag>
- [11] M. Misiak *et al.*, Phys. Rev. Lett. **98**, 022002 (2007) [arXiv:hep-ph/0609232].
- [12] M. Misiak and M. Steinhauser, Nucl. Phys. B **764** (2007) 62 [arXiv:hep-ph/0609241].
- [13] U. Haisch, arXiv:0805.2141 [hep-ph].
- [14] M. Iwasaki *et al.* [Belle Collaboration], Phys. Rev. D **72**, 092005 (2005) [arXiv:hep-ex/0503044].
- [15] B. Aubert *et al.* [BABAR Collaboration], Phys. Rev. Lett. **93**, 081802 (2004) [arXiv:hep-ex/0404006].
- [16] C. Bobeth, M. Misiak and J. Urban, Nucl. Phys. B **574**, 291 (2000) [arXiv:hep-ph/9910220].
- [17] H. H. Asatryan, H. M. Asatrian, C. Greub and M. Walker, Phys. Rev. D **65** (2002) 074004 [arXiv:hep-ph/0109140].
- [18] H. M. Asatrian, K. Bieri, C. Greub and A. Hovhannisyan, Phys. Rev. D **66**, 094013 (2002) [arXiv:hep-ph/0209006].
- [19] A. Ghinculov, T. Hurth, G. Isidori and Y. P. Yao, Nucl. Phys. B **685**, 351 (2004) [arXiv:hep-ph/0312128].
- [20] C. Bobeth, P. Gambino, M. Gorbahn and U. Haisch, JHEP **0404**, 071 (2004) [arXiv:hep-ph/0312090].
- [21] T. Huber, E. Lunghi, M. Misiak and D. Wyler, Nucl. Phys. B **740**, 105 (2006) [arXiv:hep-ph/0512066].
- [22] T. Huber, T. Hurth and E. Lunghi, arXiv:0712.3009 [hep-ph].
- [23] Z. Ligeti and F. J. Tackmann, Phys. Lett. B **653** (2007) 404 [arXiv:0707.1694 [hep-ph]].
- [24] T. Aaltonen *et al.* [CDF Collaboration], Phys. Rev. Lett. **100** (2008) 101802 [arXiv:0712.1708 [hep-ex]].
- [25] G. Buchalla, A. J. Buras and M. E. Lautenbacher, Rev. Mod. Phys. **68** (1996) 1125 [arXiv:hep-ph/9512380].
- [26] Q. Mason *et al.* [HPQCD Collaboration and UKQCD Collaboration], Phys. Rev. Lett. **95**, 052002 (2005) [arXiv:hep-lat/0503005]; C. Bernard *et al.* [Fermilab Lattice, MILC and HPQCD Collaborations], PoS **LATTICE2007**, 370 (2007).
- [27] B. Aubert *et al.* [BABAR Collaboration], arXiv:0804.4412 [hep-ex]; Phys. Rev. D **73**, 092001 (2006) [arXiv:hep-ex/0604007].
- [28] M. Beneke, T. Feldmann and D. Seidel, Nucl. Phys. B **612**, 25 (2001) [arXiv:hep-ph/0106067].
- [29] M. Beneke, T. Feldmann and D. Seidel, Eur. Phys. J. C **41** (2005) 173 [arXiv:hep-ph/0412400].

- [30] A. Ali, G. Kramer and G. h. Zhu, Eur. Phys. J. C **47** (2006) 625 [arXiv:hep-ph/0601034].
- [31] P. Ball and R. Zwicky, Phys. Rev. D **71** (2005) 014029 [arXiv:hep-ph/0412079].
- [32] S. Adler *et al.* [E787 Collaboration], Phys. Rev. D **77** (2008) 052003; V. V. Anisimovsky *et al.* [E949 Collaboration], Phys. Rev. Lett. **93** (2004) 031801 [arXiv:hep-ex/0403036].
- [33] M. Antonelli *et al.* [FlaviaNet Working Group on Kaon Decays], arXiv:0801.1817 [hep-ph] and online update at <http://www.lnf.infn.it/wg/vus/> from Rare K decays and Decay Constants.
- [34] J. Brod and M. Gorbahn, arXiv:0805.4119 [hep-ph].
- [35] A. J. Buras, M. Gorbahn, U. Haisch and U. Nierste, JHEP **0611**, 002 (2006) [arXiv:hep-ph/0603079]; Phys. Rev. Lett. **95**, 261805 (2005) [arXiv:hep-ph/0508165].
- [36] G. Isidori, F. Mescia and C. Smith, Nucl. Phys. B **718**, 319 (2005) [arXiv:hep-ph/0503107].
- [37] F. Mescia and C. Smith, Phys. Rev. D **76**, 034017 (2007) [arXiv:0705.2025 [hep-ph]].
- [38] A. J. Buras, Phys. Lett. B **566**, 115 (2003) [arXiv:hep-ph/0303060].
- [39] C. Bobeth, M. Bona, A. J. Buras, T. Ewerth, M. Pierini, L. Silvestrini and A. Weiler, Nucl. Phys. B **726** (2005) 252 [arXiv:hep-ph/0505110].
- [40] U. Haisch and A. Weiler, Phys. Rev. D **76**, 074027 (2007) [arXiv:0706.2054 [hep-ph]].
- [41] K. S. Babu and C. F. Kolda, Phys. Rev. Lett. **84** (2000) 228 [arXiv:hep-ph/9909476].
- [42] G. Isidori and A. Retico, JHEP **0111** (2001) 001 [arXiv:hep-ph/0110121].
- [43] W. Altmannshofer, A. J. Buras and D. Guadagnoli, JHEP **0711** (2007) 065 [arXiv:hep-ph/0703200].
- [44] P. Gambino, M. Gorbahn and U. Haisch, Nucl. Phys. B **673** (2003) 238 [arXiv:hep-ph/0306079].
- [45] M. Gorbahn and U. Haisch, Nucl. Phys. B **713**, 291 (2005) [arXiv:hep-ph/0411071].
- [46] G. Buchalla, G. Isidori and S. J. Rey, Nucl. Phys. B **511** (1998) 594 [arXiv:hep-ph/9705253].
- [47] S. J. Lee, M. Neubert and G. Paz, Phys. Rev. D **75** (2007) 114005 [arXiv:hep-ph/0609224].
- [48] T. Huber, T. Hurth and E. Lunghi, arXiv:0807.1940 [hep-ph].
- [49] P. Ball and R. Zwicky, JHEP **0110** (2001) 019 [arXiv:hep-ph/0110115].
- [50] A. Ali, P. Ball, L. T. Handoko and G. Hiller, Phys. Rev. D **61** (2000) 074024 [arXiv:hep-ph/9910221].
- [51] G. Hiller and F. Kruger, Phys. Rev. D **69**, 074020 (2004) [arXiv:hep-ph/0310219].
- [52] R. J. Hill, T. Becher, S. J. Lee and M. Neubert, JHEP **0407** (2004) 081 [arXiv:hep-ph/0404217].
- [53] U. Egede, T. Hurth, J. Matias, M. Ramon and W. Reece, arXiv:0807.2589 [hep-ph].
- [54] P. Ball and R. Zwicky, Phys. Rev. D **71** (2005) 014015 [arXiv:hep-ph/0406232].
- [55] G. Buchalla, G. Hiller and G. Isidori, Phys. Rev. D **63** (2001) 014015 [arXiv:hep-ph/0006136].
- [56] P. Colangelo, F. De Fazio, R. Ferrandes and T. N. Pham, Phys. Rev. D **73** (2006) 115006 [arXiv:hep-ph/0604029].
- [57] M. Misiak, private communication.
- [58] W. M. Yao *et al.* [Particle Data Group], J. Phys. G **33**, 1 (2006), and online update at <http://pdg.lbl.gov/>
- [59] N. Tantalo, arXiv:hep-ph/0703241; S. Hashimoto, hep-ph/0411126; D. Becirevic, hep-ph/0310072.

- [60] P. Gambino, U. Haisch and M. Misiak, Phys. Rev. Lett. **94**, 061803 (2005) [arXiv:hep-ph/0410155].
- [61] A. Ishikawa *et al.*, Phys. Rev. Lett. **96** (2006) 251801 [arXiv:hep-ex/0603018].
- [62] K. Abe *et al.* [Belle Collaboration], arXiv:hep-ex/0410006.
- [63] B. Aubert [The BABAR Collaboration], arXiv:0807.4119 [hep-ex].
- [64] C. Bobeth, G. Hiller and G. Piranishvili, JHEP **0712** (2007) 040 [arXiv:0709.4174 [hep-ph]].
- [65] K. F. Chen *et al.* [BELLE Collaboration], Phys. Rev. Lett. **99** (2007) 221802 [arXiv:0707.0138 [hep-ex]];  
B. Aubert *et al.* [BABAR Collaboration], Phys. Rev. Lett. **94** (2005) 101801 [arXiv:hep-ex/0411061].
- [66] J. Nix *et al.* [E391a Collaboration], Phys. Rev. D **76** (2007) 011101 [arXiv:hep-ex/0701058].